



**HAL**  
open science

## Considering the polarization of the oxygen thermospheric red line for space weather studies

Jean Lilensten, Cyril Simon, Mathieu Barthelemy, Joran Moen, Roland  
Thissen, D. A. Lorentzen

► **To cite this version:**

Jean Lilensten, Cyril Simon, Mathieu Barthelemy, Joran Moen, Roland Thissen, et al.. Considering the polarization of the oxygen thermospheric red line for space weather studies. Space Weather: The International Journal of Research and Applications, 2006, 4 (11), pp.S11002. 10.1029/2006SW000228 . insu-00357259

**HAL Id: insu-00357259**

**<https://insu.hal.science/insu-00357259>**

Submitted on 5 Mar 2021

**HAL** is a multi-disciplinary open access archive for the deposit and dissemination of scientific research documents, whether they are published or not. The documents may come from teaching and research institutions in France or abroad, or from public or private research centers.

L'archive ouverte pluridisciplinaire **HAL**, est destinée au dépôt et à la diffusion de documents scientifiques de niveau recherche, publiés ou non, émanant des établissements d'enseignement et de recherche français ou étrangers, des laboratoires publics ou privés.

# Considering the polarization of the oxygen thermospheric red line for space weather studies

Jean Lilensten,<sup>1</sup> Cyril Simon,<sup>2</sup> Mathieu Barthélémy,<sup>1</sup> Joran Moen,<sup>2</sup>  
Roland Thissen,<sup>3</sup> and D. A. Lorentzen<sup>4</sup>

Received 14 February 2006; revised 12 June 2006; accepted 15 June 2006; published 21 November 2006.

[1] Space weather thermospheric monitoring requires real-time and large-scale measurements. In order to monitor the thermospheric variations due to geomagnetic activity, one relies mostly on the measurements of the intensity of the atomic oxygen green line and on the indirect measurement of the total electron content. These two parameters do not allow retrieving the full characteristics of the thermosphere, and a third proxy is required, for example, in orbitography. We propose to use the polarization of the atomic oxygen red line to fulfill this requirement. The first measurements of the polarization of thermospheric nightglow lines have been performed in the first part of the twentieth century and especially during the last International Geophysical Year. Amongst the oxygen visible lines, only the red one seems to be potentially polarized. However, there exists a disagreement between the different measurements. At the origin of the polarization, there is always a dissymmetric mechanism. It triggers either an emission process, a light scattering, or, in the case of the oxygen red line, a collision mechanism. This paper reviews the different experiments performed in the past and proposes to explore this matter with modern facilities. If successful, this investigation could lead to a systematic reanalysis of the previous red line interferometric measurements.

**Citation:** Lilensten, J., C. Simon, M. Barthélémy, J. Moen, R. Thissen, and D. A. Lorentzen (2006), Considering the polarization of the oxygen thermospheric red line for space weather studies, *Space Weather*, 4, S11002, doi:10.1029/2006SW000228.

## 1. Introduction: On the Need of New Observations to Monitor the Thermosphere in the Frame of Space Weather

### 1.1. Position of the Problem

[2] When an object (spacecraft, debris, etc.) travels through an atmosphere it experiences a drag force in a direction opposite to the direction of its motion. In a first simple approach, this drag force is given by

$$D = \frac{1}{2} \rho v^2 A C_d \quad (1)$$

where  $\rho$  is the thermospheric density,  $v$  is the object velocity,  $A$  is the object cross-section area and  $C_d$  is a drag coefficient of the order of 2. The reduction in the period  $P$  of the spacecraft due to atmospheric drag is given by

$$\frac{dP}{dt} = -3\pi a \rho \frac{A C_d}{m} \quad (2)$$

where  $a$  is the semimajor axis of the spacecraft trajectory and  $m$  is the mass of the object. The evaluation of the drag force depends on the knowledge of the thermosphere density. This usually comes from a model. The sources of variations of the thermosphere are mainly X-rays and EUV fluxes, particle precipitation and  $E$  fields. The physical processes involve photoabsorption, particle collisions, Joule heating and frictional heating. For space weather, the main consequence (amongst other phenomena) of an increase of the input energy is a dilation of the thermosphere: the density may increase by a factor of 10 at the altitude of the International Space Station.

[3] Most of the perturbation sources (X rays, EUV fluxes, and particle precipitation) are badly known, monitored, predicted, and modeled. Thanks to the Superdarn facility, the knowledge of the electric field has been improved in the recent years (<http://superdarn.jhuapl.edu/>). However, this measurement depends on the presence of irregularities in the ionosphere. When there are no irregularities, a model is used to fill the gaps.

[4] It is therefore not surprising that the models fail in reproducing the real time atmosphere, especially at high latitude and during magnetic perturbations. This implies a large uncertainty on the position of the spacecraft [Nicholas *et al.*, 2000]. Since the actual goal is to reach a precision

<sup>1</sup>Laboratoire de Planétologie de Grenoble, Grenoble, France.

<sup>2</sup>Department of Physics, University of Oslo, Oslo, Norway.

<sup>3</sup>Laboratoire de Chimie-Physique, Orsay, France.

<sup>4</sup>Arctic Geophysics, University Centre in Svalbard, Longyearbyen, Norway.

of 20 km after 24 hours, there is a necessity of a permanent monitoring and adjustment of the drag equation through neutral atmosphere models. Several methods are used.

[5] The first one is a proxy approach, or use of indices, which remain basic data in space weather. Several exist to monitor the solar activity and the EUV flux variation or the geomagnetic activity at different scales. They are still impossible to bypass for long-term studies. Better indices with better space and time coverage are needed in several applications. Another approach is the technological approach. An example is given by *Nicholas et al.* [2000], where, a reference object is used to estimate the thermospheric drag, which then feeds the drag equation for the other spacecrafts. Although very efficient, this approach necessitates to have an extremely well calibrated reference instrument with a great temporal stability. There are also physical approaches, consisting in feeding models with observations. The observations are of different kinds.

### 1.1.1. UV Airglow Monitoring

[6] A spacecraft observes the airglow over a large scale. The thermosphere is adjusted in glow models until the computations fit the observations. This method is at work at the 55th squadron for space weather. Although it is very efficient, it is also very expensive and only works along the spacecraft orbit.

### 1.1.2. Temperature Monitoring

[7] The neutral exospheric temperature is measured (for example, using an incoherent scatter radar) and compared to the exospheric temperature given by empirical models [*Lathuillère et al.*, 2002]. The total density is then extracted from the model to calculate the drag force. This method is not well suited to space weather studies because the measurement of the exospheric temperature is very difficult to perform and gives the state of the atmosphere only at one position.

### 1.1.3. Use of the Ionosphere as a Tracer of the Thermosphere

[8] In this case, one may use ionospheric profiles measured by incoherent scatter radars [*Blelly et al.*, 1996], or integrated parameters such as the total electron content [*Lilensten and Blelly*, 2002]. However, the fit of a single integrated parameter such as the TEC does not give a unique solution, and the method must be improved with the use of a second type of observation. This is why combined methods have been developed, such as incoherent scatter plus visible airglow (red and green lines of the atomic oxygen) [*Culot et al.*, 2004].

[9] However, the variations of the thermospheric density may be more important for orbitography purposes than its absolute value itself. In a recent work [*Culot et al.*, 2005], it has been shown that the variation of the green line intensity follows well the variation of the magnetic activity, but that the intensity of the red line does not vary in an extent that could be measured and/or modeled.

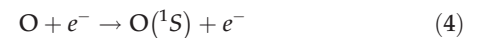
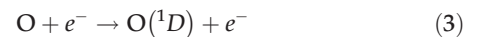
[10] There are two requirements for space weather applications. The first one is real-time (or near-real-time) measurements. The second one is large-scale measure-

ments. As far as the thermosphere is concerned, we are then left with only two measurements fitting these constraints to monitor the effects of the geomagnetic activity on the thermosphere: (1) the TEC (ionospheric measurement) through GPS and (2) the intensity of the oxygen green line. These two parameters do not allow retrieving the full characteristics of the thermosphere [*Lilensten and Blelly*, 2002]. It is therefore important to find a new proxy of the thermospheric variability. We propose to use the polarization of the atomic oxygen red line as a third hint to explore this issue.

## 1.2. Thermospheric Oxygen Emissions

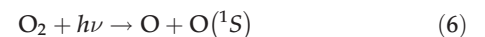
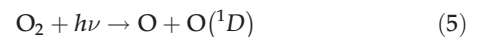
[11] In the ionospheric *F* region, typically from 150 to 400 km, the main source of ionization is the EUV radiation below 90 nm. This region is collisional, with elastic as well as inelastic collisions. It also hosts chemical reactions including both neutral and ionized species. In the nightside ionosphere, the particle precipitations have similar effects than the EUV flux in the dayside. There, electrons and protons originating in the solar wind and accelerated in the magnetosphere constitute the main excitation, dissociation, heating and ionization source. Transport phenomena linked to the presence of the Earth's magnetic field are important in both cases.

[12] The thermospheric emissions come from the deactivation of excited atoms, molecules or ions. In the *F* region, the atomic oxygen is one of the main contributors to the glow in the visible light. Its main emissions correspond to the transitions from state  $^1S$  to  $^1D$  and  $^1D$  to  $^3P$ . The first transition creates the green line at 557.7 nm, and the second one forms the triplet at 630.0, 636.4 and 639.2 nm, which constitutes the red line emission. The production of the excited states *D* is due to different phenomena [*Witasse et al.*, 1999, and references therein]: energetic electron impact:

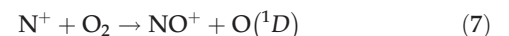


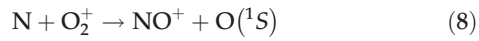
The electrons may be thermal (energy < 1 eV) or suprathermal, from photoionization or precipitation origins.

Photodissociation:



Chemical reaction with  $\text{N}(^2D)$  or  $\text{N}^+$ :





Cascade from an upper level:



Dissociative recombination with  $\text{O}_2^+$ :



The photodissociation, the chemical reactions or the cascade from upper energy levels are isotropic.

[13] It is also the case with the dissociative recombination when thermal electrons are involved, because the thermal distribution is spatially isotropic (Maxwellian). Therefore, in the diurnal case when the source is the electromagnetic EUV radiation, one does not expect any polarization of the oxygen emission. This has to be confirmed by experiments. In the following, we will only deal with the nocturnal case, when strong anisotropic sources are present.

[14] When the source is reduced to energetic particle impact, the presence of a magnetic field may impose a well collimated pitch angle. In this case, one may expect a polarized emission because the excitation source is anisotropic. This happens during nighttime with a larger probability when the energies of the incoming electrons are relatively homogeneous.

## 2. Observations: Comprehensive Review

[15] At the beginning of the twentieth century, astronomers understood that part of the nightglow is of atmospheric origin. On the one hand, the scattering of the star light cannot explain the enhancement of the glow intensity far from the zenith. On the other, only a very small part of the nightglow is concentrated on the line of sight of the Milky Way where most of the closest stars are found.

[16] With the improving spectroscopes, they came to the conclusion that the most intense line of the auroral spectrum, the green line (557.7 nm), is a permanent feature of both the nightglow and dayglow [Ångström, 1868; Campbell, 1895; Slipher, 1919]. Yntema [1909] even mentions the presence of a “permanent aurora.” In parallel, the red line (at 630 nm) is discovered by Zöllner [1870]. Its origin soon receives some interpretations [Slipher, 1919]. In 1919–1920, Fabry draws the attention on one of the main problems of the nightglow: several emissions are mixed altogether, such as the stellar background emission, the sunlight scattered by interplanetary gas or dust, and finally the atmospheric emission itself. With the goal of characterizing each contribution, Lord Rayleigh [1919] and Babcock [1919] proceed to the first measurement of the nightglow polarization with no positive result. Ten years later, Dufay

[1928, 1929] reproduces these measurements and finds a polarization rate of 2 to 4% of the nightglow in a plane that includes the solar azimuth. He concludes that about 15% of the nightglow is due to the zodiacal light. After 1925, some systematic measurements of the polarization of the sky light are performed, rapidly concentrating on individual lines. Khvostikov [1938] observes polarization rates up to 15%. These high values seem to contradict Ginsburg’s [1943] theoretical developments. Bricard and Kastler [1947a, 1947b] use a Savart and Lyot polariscope to observe the diurnal and nocturnal lines. They find no polarization.

[17] Thanks to the International Geophysical Year (IGY) in 1958, Duncan [1959] and Chamberlain [1959] show results on the polarization of the oxygen red line. Their results are detailed hereafter. They differ considerably, originating in a scientific dispute.

[18] Since then, very few studies have been performed. Chamberlain [1974] still states the possible polarization of the red line. Some soviet studies [Nadubovich, 1977; Korobotsova, 1981; Karasheva et al., 1985] mention a polarization rate ranging between 18 and 56%, depending on the geophysical condition. None of these early studies have yet been confirmed.

### 2.1. Early Results

#### 2.1.1. First Hypothesis (1943)

[19] In 1929, Dufay shows that the nightglow is partially polarized. Khvostikov [1938] concludes that the polarization is that of individual lines ( $\lambda = 557.7 \text{ nm}$ ,  $\lambda = 630.0 \text{ nm}$ ,  $\lambda = 589.0 \text{ nm}$ ). Ginsburg [1943], pointing out the real lack of measurements, interprets the auroras as being due to electron collisions in the atmosphere. He also shows that the green line cannot be polarized because its upper state ( $^1\text{S}$ ) is not degenerated. This theoretical conclusion does not depend on the excitation mechanism. He then rules out the green line as a potential cause of the observed glow polarization. The red line, however, remains a good candidate because the transition is mostly magnetic dipolar with a transition energy proportional to the magnetic momentum and to the magnetic field. Ginsburg’s developments were however limited by the fact that at that time, there was no theoretical explanation of the collision induced polarization.

#### 2.1.2. Bricard and Kastler [1947a, 1947b]

[20] This study has been performed over three years. The authors used a Savart fringe polariscope updated by Lyot [Bricard and Kastler, 1947a]. This device includes two birefringent elements with their optical axis at  $90^\circ$  from each other, and making an angle of  $45^\circ$  with the sides. The polarization is simply measured by adding a glass slide at the front of the polariscope. This filter is inclined, so as to introduce a polarization equal and orthogonal to that of the measured beam light. It allows killing the interference fringes and computing the polarization rate of the beam. Lyot improved the system by noticing that the human eye is more sensitive to the light itself than to its extinction. He then replaced the analyzer by a Wollaston prism

which allows studying the contrast between two polarized components.

[21] Thanks to this improvement, the two authors could measure polarization rates of the order of 0.1%, which is remarkable considering that the process was purely visual. However, positive results only applied to the sodium yellow line [Bricard and Kastler, 1950]. The authors noticed no polarization when observing the oxygen red and green lines [Bricard and Kastler, 1947b].

### 2.1.3. Duncan [1959]

[22] The Bricard and Kastler results ended up the studies for about 10 years, until the Australian physicist R. A. Duncan performed a long series of measurements in 1957 in the frame of the International Geophysical Year. He measured the polarization of the red line in middle and low-latitude auroras during one year, which resulted in only 30 nights of observations. On 8 July 1958, he measured a polarization rate of 30%. Since it was only measured once over 30 nights, it cannot be attributed to secondary effects such as the atmospheric scattering. He interpreted this result as being due to the precipitation of low-energy electrons (smaller than 10 eV) colliding with the neutral atmosphere. The helicoidal motion of the electrons around the magnetic field line imposes a precession symmetrical around the field line to the excited atoms, because its lifetime is long (110 s). Following this theory, no polarization can occur parallel to the magnetic field line. Indeed, an excited oxygen atom  $^1D_2$  will radiate in a direction perpendicular to the magnetic dipole from which it originated. The only way to detect the polarization is therefore to look perpendicularly to the magnetic field line. From mathematical considerations, Duncan concludes that the electrons at the origin of the polarization must have a gyration motion rather than a longitudinal one. Since then, these results have never been confirmed. Instead, Chamberlain [1959] put some doubt on Duncan's semiclassical interpretation.

## 2.2. Recent Developments

[23] No measurement of the polarization of the oxygen red line has been performed for the last half century. However, it has been recently modeled. The authors of this paper have developed an ionospheric code over the last decade [Lilensten and Blelly, 2002]. From a given atmosphere and a given precipitating electron flux, this code allows to compute the suprathermal electron distribution at each altitude, energy and pitch angle by solving a multistream stationary kinetic Boltzmann equation. Using the outputs of this model, Kazantsev *et al.* [1999] theoretically showed that the oxygen red line could have a polarization rate of about 30%, in agreement with Duncan's unique observation. This calculation remains to be confirmed experimentally.

## 3. Description of the Polarizing Mechanisms

[24] The polarization originates necessarily in a dissymmetry. The dissymmetry can affect the emission itself, or

the radiation during its way to the observer. In the natural environment, the number of processes at work decreases the sources of dissymmetry. It means that we have to be able to measure very low polarization rates in order to get some astrophysical information. Several phenomena can contribute to the dissymmetry and then to a polarization.

### 3.1. Polarization of the Emission

[25] Zeeman [1897] discovered that when an atomic spectrum is emitted by a source in the presence of a magnetic field, the spectral lines are divided into several components. The components are linearly or circularly polarized, depending on the angle between the magnetic field and the line of sight. However, in the case of the Earth, Chamberlain [1961, 1974] suggested that the geomagnetic field is not large enough to polarize the thermospheric lines. When there is no magnetic field, the Zeeman levels are degenerated but each sublevel produces a different polarization so that we have to calculate their populations. When the beams of electrons hit the atmospheric gas, there are two essential parameters of the corresponding line: the impact angle which creates the dissymmetry and the energy of the incident particle. Those two parameters allow calculating the density matrix corresponding to the population of the  $m$  sublevels. The state of polarization is entirely defined by the Stokes parameters but if we are only interested by linear polarization, the polarization rate  $P$  is the most relevant parameter,

$$P = \frac{I_{\parallel} - I_{\perp}}{I_{\parallel} + I_{\perp}} \quad (12)$$

where  $I_{\parallel}$  and  $I_{\perp}$  are the intensity of the emissions with an electric field parallel and perpendicular, respectively, to the plan that includes both the incident particles and the line of sight. Therefore the best observations should be a priori performed with a line of sight perpendicular to the magnetic field. This definition is valid if the line of sight is not parallel to the particle beam, but in this case linear polarizations are very unlikely if no other dissymmetry breaks the equivalence between the two directions perpendicular to the particle beam.

[26] The modeling of the polarization rate can be performed by ab initio calculation or from laboratory experiments. Percival and Seaton [1958] developed the ab initio calculation for an atom considering an electric dipolar transition by taking into account spin orbit coupling, considering the angular orbital momentum of the ground level as null, and considering that the excitation potential does not depend of spin coordinates.

[27] The polarization rate is positive when  $I_{\parallel} > I_{\perp}$ . In the classical approach, this cannot happen when the velocities are small, because a slow particle creates temporally an electric dipole parallel to the beam. If the velocity (and therefore the energy) of the incident particle is high, the inverse happens: the dipole is perpendicular to the inci-

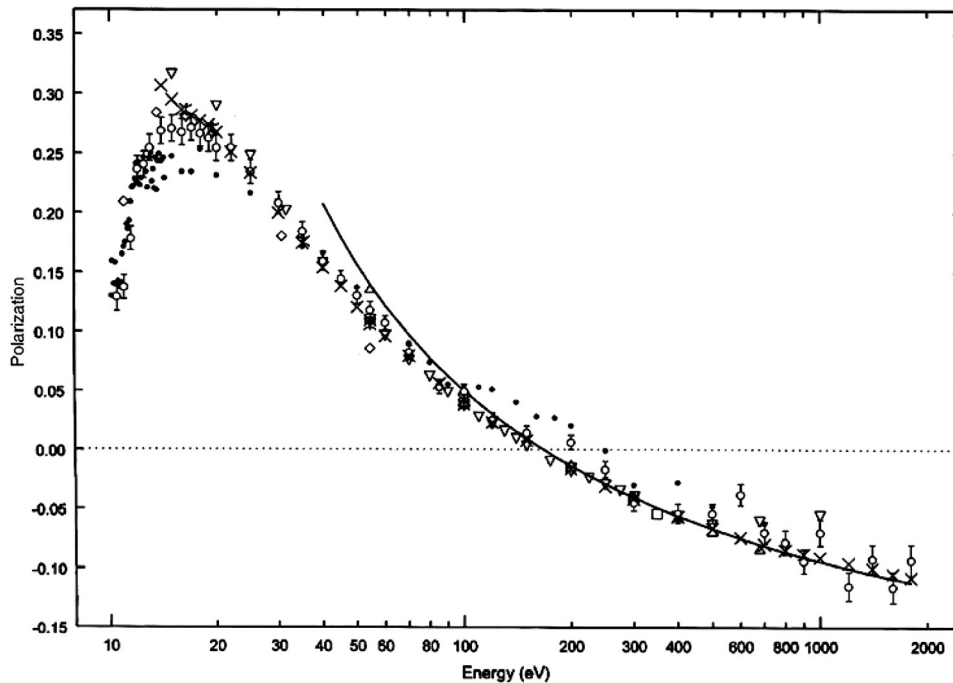


Figure 1. Experimental and theoretical values for the polarization of Lyman  $\alpha$  radiation from atomic hydrogen excited by electron impact over the energy range from threshold to 1800 eV. The dotted line representing zero polarization is added for clarity. (Reprinted from work by *James et al.* [1998]. Copyright 1998 by the American Physical Society).

dent beam. However, the classical view is insufficient to describe quantitatively the polarization phenomenon. We have to calculate the density matrix of the system. In those cases the semi classical formalism using the Bethe theory could be used [McFarlane, 1974]. It is also possible to use the quantum formalism and to calculate the density matrix of the system [Fineschi and degl'Innocenti, 1992].

[28] However, the ab initio calculations are particularly complex and do not provide sufficient precision. Therefore it is necessary to proceed to laboratory measurements. Some have been made on the Lyman alpha and beta lines for atomic hydrogen for energies ranging from the threshold to 1000 eV [James et al., 1998, 2002] and for the helium 1 snp series [Merabet et al., 1999]. In each case, the curve of the polarization rate shows similar profiles (Figure 1).

[29] We observe a positive increasing polarization just above the threshold. It reaches a maximum (for example at 15 eV in the Lyman alpha case.) and decreases above. Around several hundred eV the polarization tends to zero (at around 150 eV in the Lyman alpha case) and to a negative asymptote at high energies. In the decreasing part of the curve, the results are similar with the Bethe theory [James et al., 1998, 2002; Merabet et al., 1999] (Figures 2 and 3).

## 3.2. Polarization During Transfer: Diffusion Phenomena

### 3.2.1. Rayleigh and Thomson Scattering: Polarization of the Continuum

[30] The Rayleigh scattering is well known, as being responsible for the blue color of the sky. The scattering of the sunlight by the atmospheric molecules is much more efficient in the blue than in the red because the scattered power is inversely proportional to the fourth power of the wavelength. The emitted light is linearly polarized perpendicularly to the plane that contains both the Sun-Earth axis and the scattering particle direction. The polarization rate  $P$  is

$$P = \frac{C^2 - C^2 \cos^2 \alpha}{C^2 + C^2 \cos^2 \alpha} = \frac{\sin^2 \alpha}{1 + \cos^2 \alpha} \quad (13)$$

where  $C$  is the amplitude of the wave, which is independent from the wavelength and  $\alpha$  is the angle between the Sun-Earth axis and the line of sight. When this angle is  $0^\circ$ , the polarization rate is null and the light is unpolarized. When  $\alpha$  is equal to  $90^\circ$ , the polarization rate is 1; that is, the light is totally polarized.

[31] The polarization due to the Rayleigh scattering is used by several animals such as bees, ants or crayfishes [Wehner, 1976] to find their direction. In the case of

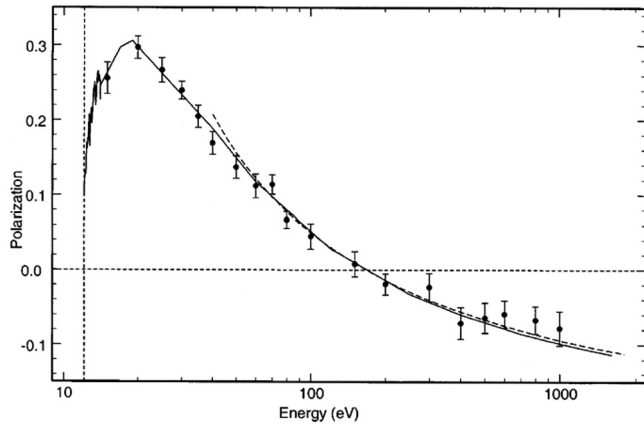


**Figure 2.** Experimental (solid circles) and theoretical values for the polarization of Lyman  $\beta$  radiation from atomic hydrogen excited by electron impact over the energy range from threshold to 1600 eV. The dashed horizontal line representing zero polarization is added for clarity (Reprinted from work by *James et al.* [1998]. Copyright 1998 by the American Physical Society).

polarimetric measurements, Rayleigh scattering has to be taken into account and thermospheric lines must be separated from the continuum of the blue sky in order to deduce their correct polarization. Moreover, it is necessary to take into account the multiple scattering. Combined with the tangential polarization of the primary scattering, the secondary scattering introduces a mostly vertical polarization which cannot be seen in the sunward direction. When looking toward the sun, the neutral point (with a null polarization rate) is called the Brewster point. In the nadir, it is called the Babinet point. Therefore it is much easier to proceed with nighttime observations. However, even the moonlight is polarized [*Dufay*, 1928, 1929; *Vassy*, 1956], which all the more shortens the observation windows suitable to possible measurements of the red line polarization.

[32] When the scattering particle is a free electron, one faces a Thomson scattering. It is at work essentially in hot atmospheres, such as the solar corona. The induced polarization is comparable to the one due to the Rayleigh diffusion, with the difference that the factor  $C$  now depends on the wavelength.

### 3.2.2. Mie Scattering

[33] Water droplets are present in the Earth lower atmosphere. When the radius of the droplets is small in front of the wavelength of the light, the Rayleigh scattering applies. In the opposite case, the light is scattered through the Mie scattering. The polarization of the scattered light depends, amongst other parameters, on the shape of the droplet. It arises in a wet saturated air (fog) or in the clouds, either on water or ice droplets. When the wave propagates through the medium, the electric field of the

particles experiences a forced oscillation. The particles then behave as oscillating electric dipoles. The polarization occurs perpendicularly to the propagation of the incident wave. In our thermospheric case, the Mie scattering may be ignored because, apart from its water-originating mechanism, it does not affect individual lines.

### 3.2.3. Depolarization by Radiative Transfer

[34] The polarized light emitted after an electronic collision can be depolarized if it is resonantly diffused. In the case of solar flares, the radiative transfer has to be taken into account. It is possible in a first approximation to consider that if the polarized emitted photon is diffused once, it is depolarized. In another way it means that if the line is optically thick, it is not sure that we will keep the polarization on all the line profile. In this case we have to take into account the redistribution effects.

## 3.3. Application to the Red Oxygen Line in Auroral Region

[35] The case of the red oxygen line is particularly complex. The approximations of *Percival and Seaton* [1958] are not valid because the transition is a dipolar magnetic transition. The lifetime of the upper level  $1D$  is 110 s. However, it is the most relevant terrestrial line to study in this polarization problem. It is the most intense in the auroral spectrum and it is formed at high altitude (about 250 km). The green line could also be a good candidate, as being quite intense. However, it is an electric quadrupolar transition. For symmetrical considerations this line cannot be significantly polarized. Furthermore,

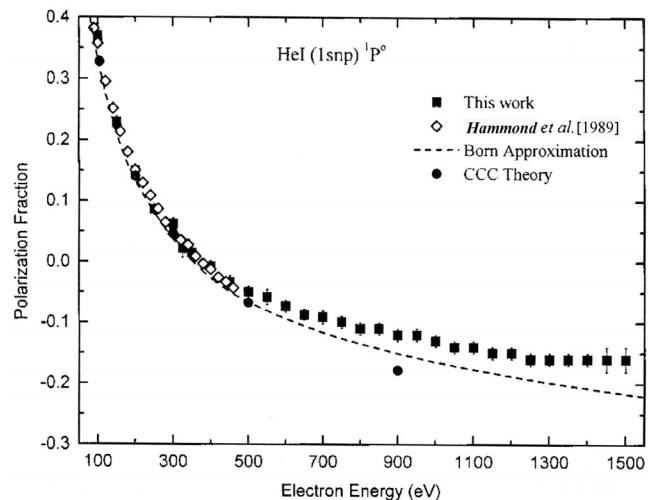


**Figure 3.** Polarization of He I (1snp stands for the transition between state  $1s$  to a  $p$  state, of any level  $n$ )  $1P0 \rightarrow (1s2)1S$  radiation as a function of electron impact energy for energies ranging from 100 to 1500 eV (Reprinted from work by *Merabet et al.* [1999]. Copyright 1999 by the American Physical Society).

the red oxygen line is the only auroral line where polarization has been observed [Duncan, 1959].

### 3.3.1. Atomic Structure and Selection Rules

[36] The red oxygen line is a triplet with wavelengths respectively of 630.0 nm, 636.4 nm and 639.2 nm. However, with no magnetic field or with a weak one, some of the three ground levels  $3P$  are degenerated. The first of these levels has a multiplicity of five ( $J = 2$ ;  $\Delta m = 0, \pm 1, \pm 2$ ; energy =  $0.0 \text{ cm}^{-1}$ , where the energy is expressed in inverse of the wavelength as is the use in atomic physics), the second has three ( $J = 1$ ;  $\Delta m = 0, \pm 1$ ; energy =  $158.3 \text{ cm}^{-1}$ ) while the last one is not degenerated ( $J = 0$ ;  $\Delta m = 0$ ;  $E = 227.0 \text{ cm}^{-1}$ ). The excited level ( $^1D$ ) is five times degenerated ( $J = 2$ ;  $\Delta m = 0, \pm 1, \pm 2$ ). The selection rules allows only for  $\Delta m = 0, \pm 1$  for a magnetic dipolar transition. If  $\Delta m = 0$ , the polarization is linear and the electric field is oriented parallel to the magnetic field. If  $\Delta m = +1$  we then get a right circular polarization, and if  $\Delta m = -1$ , we get a left circular polarization. Since we consider a magnetic dipolar transition, the problem could theoretically correspond to the quantum calculation of *Fineschi and degl'Innocenti* [1992] which allows non electric dipolar transitions. However, the presence of this triplet does not fit the frame usually defined for the calculation of the statistical equilibrium. In such calculations, one considers only the equilibrium of the upper level, which implies a nonpolarized ground level. This is not the case for two of the three lines of the triplet.

### 3.3.2. Depolarization and Dynamic of the System

[37] In the case of the red line, there is no radiative transfer depolarization; the red line is optically thin in the terrestrial atmosphere. Two effects still may depolarize the line. The first one is due to the long lifetime of the excited state. During the 110 s, the oxygen atom can collide with other atoms. In this case, we can lose the history of the excitation process and get a redistribution of the levels  $m$ . It is important to notice that the depolarizing collisions have very large impact parameters because they follow the Van der Waals interaction potential [*degl'Innocenti and Landolfi*, 2004]. The second one is the effect of the secondary electrons, which are isotropically produced through primary electron impact. Because of the isotropy, they cannot produce any polarization.

[38] Following *degl'Innocenti and Landolfi* [2004], the global dynamics of the oxygen atoms could play a role in the polarization problem. In such case, the approximation consisting of the separation of the density matrix from the velocity distribution is not valid and polarization could appear from the dynamics of the system. Then, the polarization of the red line must be compared to the polarization of allowed transition of the oxygen atomic system which have very large Einstein coefficients. In this case the triplet at 130.2, 130.4 and 130.6 nm is a good candidate. There Einstein coefficients are of the order of  $10^8 \text{ s}^{-1}$  and the ground levels are identical to the red line level.

### 3.3.3. Geometrical Problem

[39] The incident electrons have a gyration motion around the magnetic field lines. There is an angle between the field line and the particles beam. This angle depends on the energy of the particles through the conservation of the energy and the conservation of the first adiabatic invariant  $\mu = mv^2/2B_{\parallel}$  where  $m$  is the particle mass,  $v$  is its velocity, and  $B_{\parallel}$  is the parallel magnetic field intensity. Therefore there is a cylindrical symmetry around the field line. Globally the components of the velocity perpendicular to the magnetic field line should cancel out and the only component from which polarization could be expected should be the parallel one. If the cylindrical symmetry is not respected or if the distribution of energy of the electron is too broad, then we will get a global depolarization of the line. To our knowledge, there is not any theoretical calculation, nor laboratory measurement giving the polarization rate for a monodirectional beam of electrons.

## 4. New Experiment During IHY: Tribute to Duncan

[40] From the previous consideration, we are planning to perform a set of polarization measurements. One is a laboratory measurement using an atomic oxygen source, coupled to an electron gun and a polarimeter/photon counter device; the second one is a thermospheric experiment with a photometer. These two aspects are described hereafter.

[41] These experiments are scheduled to be run during the next International Heliophysical Year (IHY). That is important since the first (and only) observations were made during the 1958 IGY: our new measurements will then constitute an original tribute to this very fruitful year and especially to the pioneering work by Duncan. Funding agencies include the University UNIS at Svalbard (Norway) and the CNRS (France).

### 4.1. Description of the Polarization Laboratory Experiment

[42] In order to assess the validity of the various theoretical models describing the polarization and depolarization of the atomic oxygen red line, we will construct an experimental setup in order to measure the amount of polarization of the light emitted specifically by the  $^1D$  excited state of atomic oxygen after production by electron impact. In order to fulfill this objective, we will (1) produce a jet of ground state atomic oxygen, (2) excite it by collision with a collimated electron beam of known kinetic energy, and (3) detect the photons emitted and measure their polarization, the latter being performed at various distances (i.e., time) from the excitation region.

[43] The experiment (Figure 4) will be performed in a high vacuum chamber, in which we can fit a commercial device based on a RF discharge in low-pressure plasma, which has been optimized to fragment efficiently atmo-

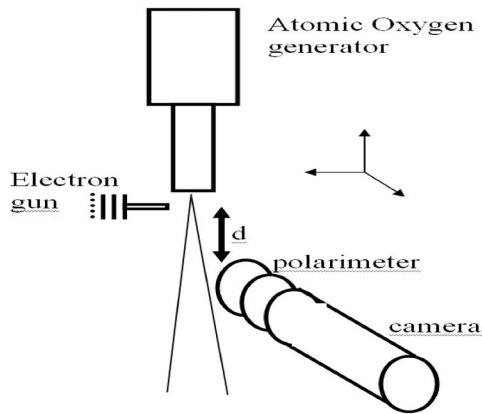


Figure 4. Description of the laboratory experiment (see text).

spheric molecules such as nitrogen or oxygen. This tool allows producing up to 10% atomic oxygen, which escapes from the plasma as an effusive beam. Previous characterization measurements by photoionization have shown that the atomic oxygen produced is predominantly (>90%) in its ground electronic state. The exhaust pipe of the device is constituted of series of channels that confine the atomic to preferential orientation, and somewhat limit the effusive beam divergence. The velocity of atomic fragments is not known with great accuracy, but presents the characteristics of an effusive beam, at a temperature lower than 500°C. We will couple, at the exit of the source a small electron gun based on a heated filament and a stack of electrodes, in order to cross the beam of effusive oxygen atoms with a collimated electron beam, the kinetic energy of which can be easily varied from 4 to 100 eV. This gun is optimized for high current intensity to the cost of energy resolution, which is not expected to be better than 1 eV, still good enough for this prospective study. The collisions with the collimated electrons will eventually induce the production of the  $^1D$  excited state of oxygen. This process should produce an oriented population of states, similarly to what is proposed in the stratosphere. Therefore, along the path of the beam, the excited atoms should emit polarized photons. These will be detected perpendicularly to the electron beam axis by a photon counter, after passing through a visible light polarimeter, and an interferometer filter, optimized for the 630–639 nm wavelength window.

[44] Authors expect to face problems associated to small signal as the emissions to be detected may very well be negligible in front of background emissions in the same wavelength window coming either directly from the plasma, or from atoms in their  $^1D$  excited state following a path identical to the ground state. This is why we plan to modulate the electron intensity by acting on the lens in

front of the electron gun, in order to disentangle the small signal from the background.

[45] The very long lifetime of the excited state (110 s) is a guarantee that along the observable path (up to 20 cm), the photon flux should be almost constant, and this will be an excellent calibration for measuring beam expansion, and neutral density along the path. Therefore, by moving the observation focus along the oxygen path, we will be able to follow the decrease of the polarization due to the collisional quenching, as described in section 4.3.2.

#### 4.2. Description of the Polarization Photometer

[46] In order to facilitate polarization measurements of the 630.0 nm [OI] auroral emission line we will develop a steerable polarization photometer (SPP) to complement the existing meridian scanning photometer (MSP) and the all-sky imaging photometer (ASIP) at Longyearbyen, Svalbard. The new photometer will be mounted on a steerable platform, that can rotate  $\sim 200^\circ$  in azimuth and  $180^\circ$  in elevation, i.e., a flexible system that can point in any direction or sweep in any plane. A one inch photometer tube will be fitted with a front lens, a narrow band 630.0 nm interference filter, and furthest out, a linear polarization filter mounted in a rotator that can turn  $360^\circ$  about its polarization axis. The sampling rate will be 20 counts per second. With the photometer fixed at one position, we will perform  $72 \times 1$  s measurement while stepping the polarization in 50 steps from  $0^\circ$  to  $360^\circ$ . Assuming that the polarization filter is symmetric about  $180^\circ$  we can achieve two complete polarization measurements within the excitation state life time of the O1D emission. After one cycle with the polarization wheel we can steer the photometer toward a new direction. The smartest approach to ensure that we keep pointing at active auroras is to perform measurements in the scan plane of the meridian scanning photometer. The MSP will provide us the elevation angle of the intensity maximum approximately four times per minute. This will allow routine measurements of the possible polarization effect. Variation in IMF and subsequent latitudinal movement of the auroral activity will ensure that we get polarization measurements at various angles with the magnetic field [Sandholt *et al.*, 1998].

#### 5. Conclusion

[47] The polarization of the oxygen red line has not been measured since half a century. At that time, the results did not allow to firmly conclude on its existence. A unique observation held during the last International Geophysical Year states a polarization rate of 30% [Duncan, 1959]. A unique recent computation shows that this is theoretically feasible [Kazantsev *et al.*, 1999]. Today, it seems possible to answer this still open question, by use of the modern sensitive remote sensing facilities, photometers or interferometers. If the red line happens to be polarized, one could deduce from this polarization some characteristics

of the precipitating particles that are still out of reach by any long-term measurements, such as their distribution function. If the polarization turns to be detectable and to faithfully represent the geomagnetic activity, it would constitute a very good and easy-to-measure parameter for space weather applications.

[48] This work also opens a new perspective for planetary atmospheres. The Jovian case is particularly rich because of the complex structure of its magnetosphere. However, it will be necessary to answer several problems. The first one is that the wavelength domain (H Lyman series and Lyman and Werner band for H<sub>2</sub> between 90 nm and 170 nm or the helium line at 58.4 nm) does not allow transmission measurement of the polarization. The second one is that it will be necessary to take into account the radiative transfer. The Jovian auroral lines are optically thick [Prangé et al., 1998]. Apart from these structural issues, the atoms and molecules mainly involved are on the other side well known and simpler than oxygen.

[49] **Acknowledgments.** This work is part of the European action COST 724 devoted to space weather, particularly in the frame of its working group 2 “interaction of solar wind disturbances with the Earth,” under the leadership of J. Waterman.

## References

- Ångström, A. J. (1868), Spectrum des Nordlichts, *Pogg. Ann.*, *137*, 161–163.
- Babcock, H. D. (1919), Note on the polarization of the night sky, *Astrophys. J.*, *50*, 209–221.
- Blelly, P.-L., J. Lilénsten, A. Robineau, J. Fontanari, and D. Alcaydé (1996), Calibration of a numerical ionospheric model using EISCAT data: Effect of the neutral atmosphere and the suprathermal electrons on the ionospheric plasma structure, *Ann. Geophys.*, *14*, 1375–1390.
- Bricard, J., and A. Kastler (1947a), Emploi du polariscope Savart-Lyot pour la détection des raies du ciel nocturne et crépusculaire et l'étude de leur polarisation, *C. R. Seances Hebd. Acad. Sci.*, *224*, 1555–1556.
- Bricard, J., and A. Kastler (1947b), Etude de la polarisation de la raie verte du ciel nocturne, *Ann. Geophys.*, *3*, 308–309.
- Bricard, J., and A. Kastler (1950), Polarization des radiations monochromatiques du ciel nocturne et de la raie D crépusculaire, *Ann. Geophys.*, *6*, 286–289.
- Campbell, W. W. (1895), Note on the spectrum of the aurora borealis, *Astrophys. J.*, *2*, 162–168.
- Chamberlain, J. W. (1959), On the polarization of the oxygen red line in aurorae, *Planet. Space Sci.*, *2*, 73–75.
- Chamberlain, J. W. (1961), *Physics of the Aurora and Airglow*, *Int. Geophys. Ser.*, vol. 2, Elsevier, New York.
- Chamberlain, J. W. (1974), Polarization of the airglow emission  $\lambda 6300$  in an artificially heated ionosphere, *J. Geophys. Res.*, *79*, 1239–1241.
- Culot, F., C. Lathuillère, and J. Lilénsten (2004), The OI 630 and 557.7 nm dayglow measured by WINDII and modeled by TRANSCAR, *Ann. Geophys.*, *22*, 1–14.
- Culot, F., C. Lathuillère, and J. Lilénsten (2005), Influence of geomagnetic activity on the O I 630.0 and 557.7 nm dayglow, *J. Geophys. Res.*, *110*, A01304, doi:10.1029/2004JA010667.
- degl'Innocenti, E., and M. Landolfi (2004), *Polarization in Spectral Lines*, Springer, New York.
- Dufay, J. (1928), Recherches sur la lumière du ciel nocturne, *Bull. Obs. Lyon*, *10*(9), 1–188.
- Dufay, J. (1929), Spectre, couleur et polarisation de la lumière du ciel nocturne, *J. Phys. Radium*, *6*(10), 219–240.
- Duncan, R. A. (1959), Polarization of the red oxygen auroral line, *Planet. Space Sci.*, *1*, 112–120.
- Fineschi, S., and E. L. degl'Innocenti (1992), Electron impact polarization of atomic spectral lines. I: A general theoretical scheme, *Astrophys. J.*, *392*, 337–352.
- Ginsburg, V. L. (1943), Polarization of lines in the night sky luminescence spectrum and in the spectrum of northern lights, *Dokl. Akad. Nauk SSSR*, *38*, 237–240.
- James, G. K., J. A. Slevin, D. Dziczek, J. W. McConkey, and I. Bray (1998), Polarization of Lyman- $\beta$  radiation from atomic hydrogen excited by electron impact from near threshold to 1800 eV, *Phys. Rev. A*, *57*, 1787–1797.
- James, G. K., D. Dziczek, J. A. Slevin, and I. Bray (2002), Polarization of Lyman- $\beta$  radiation from atomic hydrogen excited by electron impact from near-threshold energy to 1000 eV, *Phys. Rev. A*, *66*, 42710.
- Hammond, P., W. Karras, A. G. McConkey, and J. W. McConkey (1989), Polarization of rare-gas radiation in the vacuum-ultraviolet region excited by electron impact: Helium and neon, *Phys. Rev. A*, *40*, 1804–1810.
- Karasheva, T. T., D. K. Otorbaev, V. N. Ochkin, V. A. Rykov, and S. I. Savinova (1985), Doppler broadening of spectral lines (translated from Russian), in *Electron-Excited Molecules in a Nonequilibrium Plasma*, vol. 124, edited by N. N. Sobolev, pp. 14–75, Izdatel'stvo Nauka, Moscow.
- Kazantsev, S., A. Mikhalev, and A. Petrashen (1999), Spectropolarimetry of emission of the upper atmospheric layers: III. Polarization of the radiation of optical flares in the emission of night sky, *Opt. Spektrosk.*, *86*(4), 559–563.
- Khvostikov, I. A. (1938), Polarization of the green line of the night sky (in Russian), *Dokl. Akad. Nauk SSSR*, *21*, 322–324.
- Korobotsova, L. P. (1981), Characteristics of optical flares as observed in Yakutsk (in Russian), in *Inhomogeneities in Ionosphere*, pp. 96–102, Russ. Acad. of Sci., Moscow.
- Lathuillère, C., W. Gault, B. Lamballais, Y. J. Rochon, and B. Solheim (2002), Doppler temperatures from O1D airglow in the daylight thermosphere as observed by the WINDII interferometer on board the UARS satellite, *Ann. Geophys.*, *20*, 203–212.
- Lilénsten, J., and P. L. Blelly (2002), The TEC and F<sub>2</sub> parameters as tracers of the ionosphere and thermosphere, *J. Atmos. Sol. Terr. Phys.*, *64*, 775–793.
- McFarlane, S. C. (1974), A Bethe theory for the polarization of impact radiation, *J. Phys. B*, *7*, 1756–1771.
- Merabet, H., M. Bailey, R. Bruch, D. V. Fursa, I. Bray, J. W. McConkey, and P. Hammond (1999), Polarization study of the extreme-ultraviolet emission from helium following electron impact, *Phys. Rev. A*, *60*, 1187–1198.
- Nadubovich, Y. A. (1977), Polarization effects during flares of optical emission, aurorae and twilights (in Russian), in *Physical Phenomena in Atmosphere of High Latitudes*, pp. 40–49, Russ. Acad. of Sci., Moscow.
- Nicholas, A. C., J. M. Picone, S. E. Thonnard, R. R. Meier, K. F. Dymond, and D. P. Drob (2000), A methodology for using optimal MSIS parameters retrieved from SSULI data to compute satellite drag on LEO objects, *J. Atmos. Sol. Terr. Phys.*, *62*, 1317–1326.
- Percival, I. C., and M. J. Seaton (1958), The polarization of atomic line radiation excited by electron impact, *Philos. Trans. R. Soc. London*, *251*(990), 113–138.
- Prangé, R., D. Rego, L. Pallier, J. Connerney, P. Zarka, and J. Queinnee (1998), Detailed study of FUV Jovian auroral features with the post-COSTAR HST faint object camera, *J. Geophys. Res.*, *103*, 20,195–20,216.
- Rayleigh, Lord (J.W. Strutt) (1919), Polarization of the night sky, *Astrophys. J.*, *50*, 227–228.

- Sandholt, P. E., C. J. Farrugia, J. Moen, Ø. Noraberg, B. Lybekk, T. Sten, and T. L. Hansen (1998), A classification of dayside auroral forms and activities as a function of IMF orientation, *J. Geophys. Res.*, *103*, 23,325–23,345.
- Slipher, V. M. (1919), On the general auroral illumination of the sky and the wavelength of the chief auroral line, *Astrophys. J.*, *49*, 266–275.
- Vassy, E. (1956), *Physique de l'Atmosphère*, Elsevier, New York. (Reprinted as *Phénomènes d'Émission dans l'Atmosphère*, 1976.)
- Wehner, R. (1976), Polarized-light navigation by insects, *Sci. Am.*, *235*(1), 106–115.
- Witasse, O., J. Lilensten, C. Lathuillere, and P. L. Blelly (1999), Modeling the OI 630.0 and 557.7 nm thermospheric dayglow during EISCAT-WINDII coordinated measurements, *J. Geophys. Res.*, *104*, 24,639–24,655.
- Yntema, L. (1909), On the brightness of the sky and total amount of starlight, *Publ. Astron. Groeningen*, *22*, 1–55.
- Zeeman, P. (1897), On the influence of magnetism on the nature of the light emitted by a substance, *Astrophys. J.*, *5*, 332–357.
- Zöllner, F. (1870), Über das Spectrum des Nordlichts, *Pogg. Ann.*, *141*, 574–581.
- 
- M. Barthélémy and J. Lilensten, Laboratoire de Planétologie de Grenoble, Bât D de physique, BP 53, F-38041 Grenoble cedex, France. (jean.lilensten@obs.ujf-grenoble.fr)
- D. A. Lorentzen, Arctic Geophysics, University Centre in Svalbard, N-9170 Longyearbyen, Svalbard, Norway.
- J. Moen and C. Simon, Department of Physics, University of Oslo, P.O. Box 1048, Blindern, N-0316 Oslo, Norway.
- R. Thissen, Laboratoire de Chimie-Physique, UMR 8000 Université Paris-Sud, Bât 350, F-91405 Orsay, France.